NeuroImage: Clinical 31 (2021) 102730

Contents lists available at ScienceDirect

NeuroImage: Clinical

journal homepage: www.elsevier.com/locate/ynicl

Neurodevelopmental impairment is associated with altered white matter development in a cohort of school-aged children born very preterm

Eleanor Kennedy [a], Tanya Poppe [a,b], Anna Tottman [a], Jane Harding [a,*]

[a] Liggins Institute, University of Auckland, Auckland, New Zealand
[b] Centre for the Developing Brain, Department of Biomedical Engineering and Imaging Sciences, King's College London, London, United Kingdom

ARTICLE INFO

Keywords:
Preterm
Neurodevelopment
MRI
DTI
Brain volume
White matter
Myelination

ABSTRACT

Individuals born very preterm (<32 weeks gestation) have altered brain growth and white matter maturation relative to their full-term peers, and approximately 30% will experience neurodevelopmental impairment. We investigated the relationship between neurodevelopmental impairment and MRI measures of white matter microstructure and brain volume.

Children born before 30 weeks' gestation or who had very low birthweight (< 1500 g) underwent neurodevelopmental assessment and MRI at age 7 years as part of the PIANO study, a New Zealand-based cohort study. Fractional anisotropy (FA) and diffusivity measures were derived from diffusion tensor imaging to index white matter microstructure. Volumes were derived from T1-weighted imaging. Neurodevelopmental impairment was defined as a score < 85 on the Wechsler Intelligence Scale for Children, <5th centile on the Movement Assessment Battery for Children or a diagnosis of cerebral palsy by a paediatrician. Relationships between MRI and neurodevelopmental impairment were assessed with general linear models adjusted for sex, gestational age at birth, birthweight z-score, age at assessment, New Zealand Deprivation index score and multiplicity.

Children with neurodevelopmental impairment (n = 38) had smaller total brain, cortical grey matter and cerebral white matter volumes compared to children without neurodevelopmental impairment (n = 62) ($p < 0.05$, false discovery rate corrected), but the regional volume differences did not remain significant after adjustment for total brain volume. Lower FA and higher radial diffusivity were observed in the superior longitudinal fasciculi, uncinate fasciculi and right hemisphere corticospinal tract in children with neurodevelopmental impairment. This may reflect differences in cellular properties such as myelination or axonal packing. Neurodevelopmental impairment may reflect smaller overall brain volume and altered microstructure in white matter tracts that are important for language, cognitive and motor functioning.

1. Introduction

Approximately 11% of all live births are preterm, occurring before 37 weeks' gestation. (Blencowe et al., 2013) Preterm birth has a high economic cost, including those related to neonatal intensive care, ongoing healthcare costs and special education needs. Children born before 32 weeks' gestation (very preterm, VPT) have higher rates of neurodevelopmental disability (Blencowe et al., 2013) and greater individual estimated cost of care through the childhood years (Petrou and Khan, 2012) than those born preterm at more mature gestations, and higher rates of cerebral palsy, cognitive delay, motor delay (Pascal et al., 2018), psychiatric symptoms (Botellero et al., 2017) and social difficulties (Lund et al., 2012) than those born at term. Magnetic resonance imaging (MRI) studies show those born VPT have altered brain maturation, including brain volume (de Kieviet et al., 2012; Lax et al., 2013; El Marroun et al., 2020) and white matter microstructure. (Li et al., 2015; Travis et al., 2015) However, it is unclear which specific brain regions have altered maturation in the 30 percent of VPT children with neurodevelopmental impairment (NDI). (Blencowe et al., 2013)

Regional brain volumes have been associated with neurodevelopmental outcomes. Volumes of white matter, cortical grey matter and intracranial volume are smaller in VPT children compared to their full-term peers, and these regional volumes are positively correlated with intelligence (IQ) and motor ability. (Monson et al., 2016) Likewise smaller subcortical grey matter volumes have been associated with poorer developmental outcomes at age 2 years, (Boardman et al., 2010)

* Corresponding author at: University of Auckland, Private Bag 92019, Auckland 1142, New Zealand.
E-mail addresses: eleanor.kennedy@auckland.ac.nz (E. Kennedy), j.harding@auckland.ac.nz (J. Harding).

https://doi.org/10.1016/j.nicl.2021.102730
Received 8 March 2021; Received in revised form 10 June 2021; Accepted 12 June 2021
Available online 17 June 2021

Table 1
Descriptive characteristics of children with and without neurodevelopmental impairment.

	Without NDI n = 62	With NDI n = 38	*p* value	MRI not included in analysis n = 29	MRI included in analysis n = 100	*p* value
Birth weight (g)	965 (221)	852 (915)	0.011	914 (254)	922 (217)	0.864
Gestational age (completed weeks)	27.0 (1.7)	26.7 (2.0)	0.412	27.1 (2.1)	26.9 (1.8)	0.704
Male	28 (45)	22 (58)	0.216	19 (66)	50 (50)	0.140
Age at assessment (years)	7.2 (0.1)	7.2 (0.2)	0.422	7.2 (0.2)	7.2 (0.1)	0.276
Twins	16 (26)	10 (26)	0.955	9 (31)	26 (26)	0.591
Maternal diabetes	4 (6)	1 (3)	0.395	1 (3)	5 (5)	0.727
Antenatal steroids	58 (94)	31 (82)	0.063	28 (97)	89 (89)	0.218
Maternal ethnicity			0.409			0.224
Māori	12 (19)	13 (34)		7 (24)	25 (25)	
Pacific Island	8 (13)	6 (16)		2 (7)	14 (14)	
Asian	7 (11)	4 (11)		8 (28)	11 (11)	
European NZ/Other	34 (55)	15 (39)		12 (41)	49 (49)	
African	1 (2)	0 (0)		0 (0)	1 (1)	
Hyperglycaemia	42 (68)	29 (76)	0.359	21 (72)	71 (71)	0.882
Hypoglycaemia	26 (42)	19 (50)	0.431	11 (38)	45 (45)	0.499
Congenital anomaly	0	0	–	0	0	–
Grade III/IV IVH	1 (2)	3 (8)	0.120	3 (10)	4 (4)	0.184
Any sepsis	13 (21)	6 (16)	0.522	5 (17)	19 (19)	0.830
CRIB-II	9.6 (2.8)	10.9 (2.7)	0.024	27.1 (2.1)	26.9 (1.8)	0.704
High deprivation at assessment	18 (29)	20 (53)	0.018	13 (45)	38 (38)	0.508

Data are presented as mean (SD) (with decimal places) or number (%) (whole numbers). Continuous data are analysed by *t*-test. Categorical data are analysed by chi-square test. IVH = Intraventricular haemorrhage. CRIB-II = Clinical Risk Index for Babies. High deprivation based on worst three deciles of New Zealand Deprivation Index

Table 2
Brain volumes between children with and without neurodevelopmental impairment (n = 100).

	Without NDI	With NDI		Unadjusted for TBV		Adjusted for TBV
	Volume mm^3	Volume mm^3	Adj. mean difference mm^3	*p* value	Adj. mean difference mm^3	*p* value
eTIV	1,509,418 (144,667)	1,442,923 (162,089)	71,990 (14,939 to 129,041)	0.014	–	–
TBV	**1,250,739 (112,216)**	**1,179,264 (127,829)**	**70,264 (25,470 to 115,058)**	**0.003***	–	–
Ventricles	18,722 (12,973)	22,089 (31,614)	−3,927 (−13,359 to 5504)	0.410	−5,059 (−15,002 to 4884)	0.315
Cortical GM	**631,254 (59,611)**	**588,229 (73,132)**	**41,109 (14,735 to 67,483)**	**0.003***	2863 (−7,768 to 13,495)	0.594
Subcortical GM	56,065 (4,481)	54,088 (4,435)	2,158 (403 to 3,914)	0.017	235 (−1,094 to 1,564)	0.726
Cerebral WM	**401,497 (46,466)**	**378,174 (44,189)**	**24,157 (6,745 to 41,569)**	**0.007***	429 (−8,689 to 9,546)	0.926
Corpus callosum	3,339 (620)	3,184 (640)	93 (−147 to 333)	0.444	−47 (−282 to 189)	0.694

Analyses have been adjusted for sex, gestational age at birth, birthweight z-score, age at assessment, multiplicity, New Zealand deprivation index. NDI = Neurodevelopmental impairment; %TBV = regional volume as a percentage of total brain volume; eTIV = estimated Total intracranial volume; TBV = total brain volume excluding ventricles; GM = grey matter; WM = white matter; * still statistically supported following FDR correction including all outcomes from Table 2 and Table 3

at age 7 years (Loh et al., 2017) and in adolescence (Botellero et al., 2017) in individuals born VPT.

White matter microstructure can be indexed using fractional anisotropy (FA) and mean diffusivity (MD) derived from diffusion tensor imaging (DTI). FA describes the fraction of diffusion within a voxel that is constrained in one direction, i.e. anisotropic. (O'Donnell and Westin, 2011). It ranges in value from 0 to 1; a higher value indicates more restricted movement of water. MD relates to the molecular diffusion rate. Both parameters may be influenced by myelination, membrane permeability and the orientation, packing and distribution of fibres in the brain. (Jones et al., 2013) FA increases and MD decreases as the brain matures. (Lebel et al., 2019) There are widespread differences in FA between VPT and full-term participants at age 6 years (Young et al., 2019) and in adolescence. (Vollmer et al., 2017) Furthermore, FA in many major white matter tracts is associated with developmental outcomes such as IQ in mid-childhood (Young et al., 2019; Duerden et al., 2013; Thompson et al., 2014) and in adolescence (Vollmer et al., 2017) and motor ability at 18 months (Duerden et al., 2015) and 7 years. (Thompson et al., 2014) However, some studies have found that DTI measures do not correlate with developmental outcomes in VPT individuals, possibly because of a wide range of abilities in this group. For example, Young and colleagues (Young et al., 2018) found that at age 4 years VPT children scored within the average range on measures of IQ, language and motor ability, and that scores did not relate to DTI measures or measures of structural connectivity, despite both white matter measures being altered in VPT children compared to full term born children.

In this study, we explored the neural basis of NDI in school-aged children who were born before 30 weeks' gestation or had very low birthweight (<1500 g) and underwent MRI and neuropsychological assessment at age 7 years. We anticipated that children with NDI would have altered measures of white matter microstructure and smaller regional brain volumes compared to children without impairment. We expected lower FA in the corticospinal tract would be associated with motor impairment and lower FA in the uncinate fasciculus, superior and inferior longitudinal fasciculi would be associated with cognitive impairment. Since brain volumes typically have a positive correlation with IQ and motor functioning, we also expected smaller subcortical grey matter volumes in those with NDI.

2. Methods

2.1. Participants

Participants were drawn from the PIANO study, a New Zealand-based cohort study investigating the long-term effects of neonatal nutritional intake and tight glycaemic control (Alsweiler et al., 2012; Tottman et al., 2018; Dai et al., 2020). Participants were < 1500 g or <

Table 3
DTI measures of regional white matter tracts between children with and without neurodevelopmental impairment (n = 73).

	Without NDI	With NDI		Without NDI	With NDI		Without NDI	With NDI		Without NDI	With NDI	
	FA	FA	*p*	MD × 10^{-4}	MD × 10^{-4}	*p*	AD × 10^{-3}	AD × 10^{-3}	*p*	RD × 10^{-4}	RD × 10^{-4}	*p*
F major	0.46 (0.06)	0.45 (0.07)	0.154	8.81 (0.45)	8.99 (0.49)	0.108	1.37 (0.08)	1.39 (0.11)	0.993	6.35 (0.69)	6.52 (0.63)	0.088
F minor	0.44 (0.05)	0.43 (0.04)	0.445	8.38 (0.36)	8.53 (0.33)	0.122	1.28 (0.06)	1.29 (0.07)	0.495	6.17 (0.51)	6.36 (0.38)	0.186
L ATR	0.44 (0.03)	0.42 (0.03)	0.023	7.88 (0.40)	8.03 (0.26)	0.171	1.19 (0.06)	1.19 (0.04)	0.997	5.86 (0.39)	6.09 (0.28)	0.041
R ATR	0.44 (0.03)	0.42 (0.03)	0.025	7.87 (0.32)	8.02 (0.28)	0.117	1.19 (0.05)	1.19 (0.05)	0.949	5.84 (0.34)	6.08 (0.30)	0.023
L CAB	0.32 (0.05)	0.30 (0.04)	0.293	9.36 (0.53)	9.68 (0.65)	0.040	1.26 (0.09)	1.29 (0.08)	0.255	7.73 (0.53)	8.10 (0.65)	0.028
R CAB	0.30 (0.05)	0.29 (0.03)	0.304	9.34 (0.58)	9.44 (0.55)	0.551	1.24 (0.09)	1.24 (0.09)	0.987	7.80 (0.62)	7.97 (0.48)	0.371
L CCG	0.50 (0.05)	0.48 (0.06)	0.302	8.02 (0.48)	8.22 (0.37)	0.137	1.30 (0.07)	1.31 (0.09)	0.556	5.53 (0.59)	5.77 (0.49)	0.150
R CCG	0.46 (0.05)	0.44 (0.05)	0.244	7.95 (0.44)	8.23 (0.45)	0.075	1.23 (0.07)	1.26 (0.09)	0.408	5.75 (0.50)	6.06 (0.46)	0.080
L CST	0.56 (0.03)	0.53 (0.03)	0.048	7.79 (0.48)	7.93 (0.31)	0.197	1.33 (0.07)	1.33 (0.05)	0.762	5.04 (0.47)	5.27 (0.37)	0.082
R CST	**0.54 (0.04)**	**0.50 (0.05)**	**0.007***	7.90 (0.45)	8.15 (0.46)	0.039	1.32 (0.07)	1.32 (0.05)	0.899	**5.23 (0.49)**	**5.63 (0.62)**	**0.007***
L ILF	0.46 (0.05)	0.46 (0.04)	0.407	8.70 (0.48)	8.85 (0.35)	0.181	1.35 (0.06)	1.37 (0.07)	0.405	6.29 (0.60)	6.43 (0.38)	0.239
R ILF	0.47 (0.04)	0.44 (0.05)	0.016	8.62 (0.30)	8.90 (0.52)	0.021	1.35 (0.05)	1.35 (0.08)	0.927	**6.20 (0.39)**	**6.60 (0.60)**	**0.006***
L SLF – p	**0.44 (0.03)**	**0.40 (0.04)**	**0.002***	7.83 (0.57)	8.06 (0.39)	0.167	1.18 (0.07)	1.17 (0.05)	0.887	5.86 (0.56)	6.22 (0.45)	0.034
R SLF – p	**0.43 (0.03)**	**0.40 (0.03)**	**0.001***	7.81 (0.35)	8.06 (0.41)	0.024	1.17 (0.05)	1.17 (0.04)	0.851	**5.86 (0.36)**	**6.22 (0.46)**	**0.002***
L SLF – t	**0.46 (0.03)**	**0.43 (0.03)**	**0.001***	8.03 (0.34)	8.25 (0.40)	0.049	1.23 (0.05)	1.24 (0.05)	0.971	**5.87 (0.38)**	**6.19 (0.42)**	**0.006***
R SLF – t	**0.46 (0.03)**	**0.42 (0.03)**	**<0.0001***	**7.87 (0.36)**	**8.16 (0.41)**	**0.008**	1.21 (0.05)	1.22 (0.05)	0.608	**5.75 (0.37)**	**6.17 (0.43)**	**0.001***
L Uncinate	**0.38 (0.03)**	**0.36 (0.03)**	**0.002***	8.49 (0.34)	8.63 (0.27)	0.080	1.22 (0.04)	1.21 (0.05)	0.484	**6.66 (0.39)**	**6.89 (0.29)**	**0.007***
R Uncinate	**0.39 (0.03)**	**0.36 (0.03)**	**< 0.005***	8.53 (0.28)	8.67 (0.37)	0.107	1.23 (0.05)	1.22 (0.05)	0.099	**6.63 (0.34)**	**6.92 (0.41)**	**0.004***

Analyses have been adjusted for sex, gestational age at birth, birthweight z-score, age at assessment, multiplicity, New Zealand deprivation index. NDI = Neurodevelopmental impairment; FA = fractional anisotropy; MD = mean diffusivity; AD = axial diffusivity; RD = radial diffusivity; ATR = anterior thalamic radiation; CAB = cingulate – angular bundle; CCG = cingulum – cingulate gyrus; CST = corticospinal tract; ILF = inferior longitudinal fasciculus; SLF – p = superior longitudinal fasciculus – parietal; SLF – t = superior longitudinal fasciculus – temporal; Uncinate = uncinate fasciculus; * still statistically supported following FDR correction including all outcomes from Table 2 and Table 3

30 weeks' gestation at birth and admitted to the neonatal intensive care unit at Auckland City Hospital between December 2012 and March 2016. Infants were excluded if they were admitted after 24 h of age, had major congenital malformation, were discharged before postnatal day 7, died or were judged to be at imminent risk of death. Ethical approval was obtained from the Northern B Ethics Committee (NTY/12/05/035).

2.2. Neurodevelopmental impairment

A certified developmental assessor trained in the use of standardised tests and overseen by a Clinical Psychologist carried out assessments, which were performed in a standard sequence. The Wechsler Intelligence Scale for Children Fourth edition Australian (WISC-IV Australian, Pearson, USA) was used to assess perceptual reasoning, verbal comprehension, working memory and processing speed as well as a global measure of intelligence (full scale intelligence quotient, FSIQ). Movement Assessment Battery for Children second edition (MABC-2, Pearson, USA) provided a total motor score, consisting of measures of manual dexterity, balance and aiming and catching. Cognitive impairment was defined as WISC-IV score of < 85. Motor impairment was defined as a MABC-2 score < 5th centile or a diagnosis of cerebral palsy by a paediatrician. NDI was defined as either cognitive or motor impairment.

2.3. MRI acquisition

All MRI scans were acquired at the Centre for Advanced MRI, University of Auckland on a Siemens MAGNETOM Skyra 3 T with a 32-channel head-coil. A high resolution (0.8 × 0.8 × 0.8 mm) T1-weighted 3D volume scan was acquired for each participant using the MP-RAGE sequence with the following parameters: repetition time (TR) = 1900 ms; echo time (TE) = 2.28 ms; field of view (FOV) = 210 mm; slice thickness = 0.85 mm; flip angle = 9°. A T2 image was also acquired [TR = 3200 ms, TE = 327 ms, FOV = 240 mm, resolution 0.9 × 0.9 × 0.9 mm]. The diffusion weighted imaging (DWI) sequence was acquired on 80 slices along the anterior-posterior direction with the following parameters: resolution = 1.7 × 1.7 × 2.0 mm; TR = 12000 ms; TE = 96 ms; FOV = 250 mm; slice thickness = 2.0 mm; 26 non-collinear gradient directions; b = 0 and b pseudorandomised between 50 and 1200 s/mm^2 in increments of 50 s/mm^2 . There were 26 b-values applied in a pseudorandomised order, each associated with one direction. All children were scanned with the same sequence of b-values. This is a paediatric sequence optimised for improved signal-to-noise ratio in a paediatric population as described elsewhere (Estep et al., 2014; Murray et al., 2016).

2.4. Image processing

The volumetric T1 and T2 weighted images were processed using the Freesurfer 6.0 image analysis suite (http://surfer.nmr.mgh.harvard.edu/), as described in detail elsewhere (Dale et al., 1999; Fischl et al., 2001, 2004). The Freesurfer recon-all stream was used to classify tissues types and structures. Briefly, the pipeline includes motion correction (Reuter et al., 2010), the removal of non-brain tissue (Ségonne et al., 2004), Talairach transformation, segmentation of subcortical white matter and deep grey matter volumetric structures (Fischl et al., 2004, 2002), intensity normalisation (Sled et al., 1998), tessellation of the grey matter white matter boundary, automated topology correction (Fischl et al., 2001; Ségonne et al., 2007), and surface deformation following intensity gradients to optimally place the grey/white and grey/cerebrospinal fluid borders at the location where the greatest shift in intensity defines the transition to the other tissue class (Dale et al., 1999; Dale and Sereno, 1993; Fischl and Dale, 2000). The process has been validated against histological analysis (Rosas et al., 2002) and manual measurements (Kuperberg et al., 2003). Dual input of T1 and T2 weighted images were used to improve the system with paediatric brains

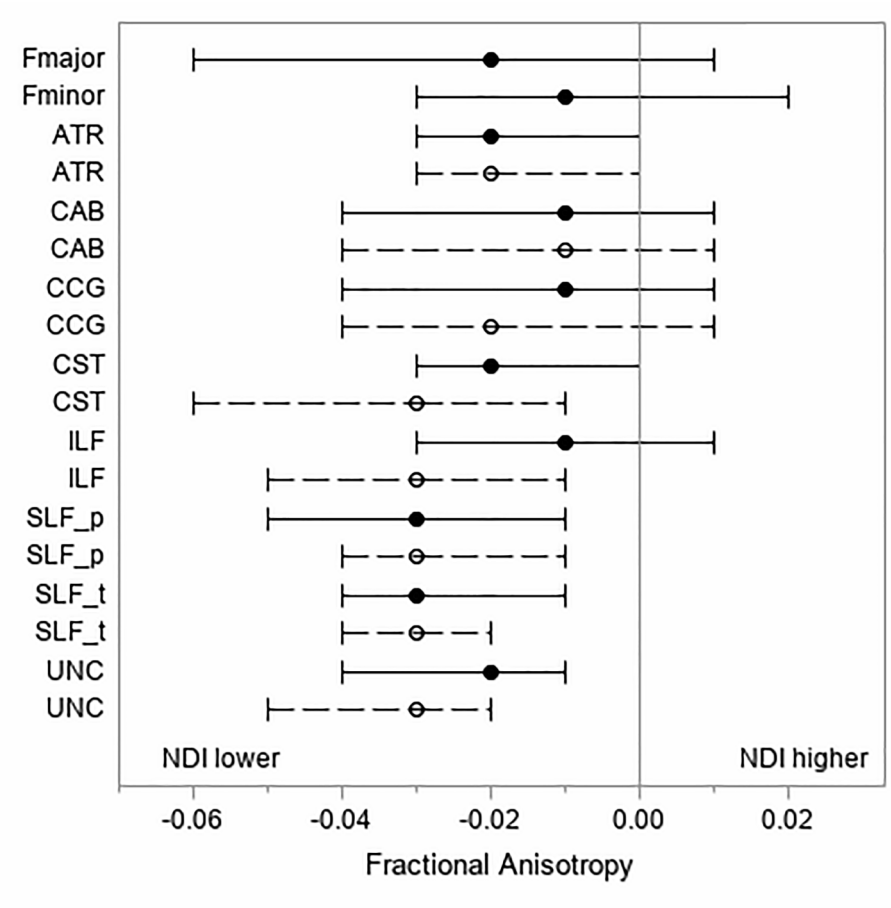

Fig. 1. Mean difference and 95% CI in fractional anisotropy (FA) between children with neurodevelopmental impairment (NDI) compared to children without NDI (reference). Solid lines/solid circles = left hemisphere; broken lines/open circles = right hemisphere; * = significant following false discovery rate correction. Fmajor = forceps major; fminor = forceps minor; ATR = anterior thalamic radiation; CAB = cingulum angular bundle; CCG = cingulum cingulate gyrus; ILF = inferior longitudinal fasciculus; SLF_p = superior longitudinal fasciculus parietal bundle; SLF_t = superior longitudinal fasciculus temporal bundle; UNC = uncinate fasciculus.

of preterm born individuals, and all images were manually corrected using the in-built Freesurfer editing packages when necessary.

All DTI images were pre-processed using Oxford Centre for Functional Magnetic Resonance Imaging of the Brain Software Library (FSL) version 5.0.10. (https://fsl.fmrib.ox.ac.uk/fsl), and the *eddycorrect* tool used to correct for motion and eddy current correction. FSL's brain extraction tool was used to brain extract the images (Smith, 2002). Automatic reconstruction of 10 (two bilateral and eight unilateral) major white matter tracts was achieved using global probabilistic tractography with anatomical priors of TRACULA in FreeSurfer 6.0, with FSL 5.0.10 (Yendiki et al., 2011). TRACULA uses individual participants' FreeSurfer recon-all anatomical segmentations and cortical parcellations. The following parameters were derived for each tract: FA, MD, radial diffusivity (RD) and axial diffusivity (AD). AD corresponds to diffusion in the principal direction parallel to the fibre and RD is the average of diffusion in the two non-principal directions perpendicular to the fibre. (Jones et al., 2013) RD has been linked with myelin loss, (Song et al., 2005, 2002) extracellular volume and axon spacing, (Schwartz et al., 2005) while it has been suggested that AD may be more related to axonal content (Song et al., 2005, 2002) and axon diameter. (Schwartz et al., 2005) Both of these measures are related to axon count and myelin volume fraction, (Schwartz et al., 2005) however, highlighting a lack of biological specificity.

2.5. Statistical analysis

Continuous data were analysed with t-tests, and categorical data were analysed with chi-square tests.

First, we compared MRI-based measures in children with and without NDI. Next, to understand the relationship between brain structure and motor and cognitive function separately, we investigated the association between MRI-based measures and WISC and MABC-2 scores. Finally, as one aim of the PIANO Study was to determine the long-term implications of neonatal hyperglycaemia, we conducted an exploratory analysis to investigate the influence of neonatal hyperglycaemia on the relationship between NDI and brain maturation. Hyperglycaemia was defined as blood glucose concentration $\geq$ 8.6 mmol/L on $\geq$ 2 measures $>$ 1 h apart, or any blood glucose concentration $\geq$ 10.1 mmol/L, and children were dichotomised as having any neonatal hyperglycaemia (n = 71) or none (n = 29).

General linear models were run with the MRI-based measures as the dependent variable. All analyses were adjusted for sex, gestational age at birth, birthweight z-score, age at assessment, NZ Deprivation index score and multiplicity. Results for the brain volumes are presented as volumes in millimetres cubed unadjusted and adjusted for TBV by including TBV as a covariate in the model. Multiple comparisons were controlled for using a False Discovery Rate (FDR) of p = 0.05 (Benjamini and Hochberg, 1995). All brain regions, both volumetric and DTI, were included in the FDR correction for each outcome. Results are described with reference to the FDR corrected findings. Sensitivity analyses were run with children with intraventricular haemorrhage (IVH) grade III or IV or with periventricular leukomalacia (PVL) excluded to remove possible effects of markers of early brain injury. For the exploratory analyses, neonatal hyperglycaemia was included as an interaction term with NDI status in additional general linear models.

3. Results

At age 7 years, 215 participants were eligible for the PIANO study and a total of 129 children took part. Twelve children declined MRI and, after exclusion of datasets due to motion (17 volumetric, 44 DTI), 100 children were included in the volumetric analysis and 73 in the DTI

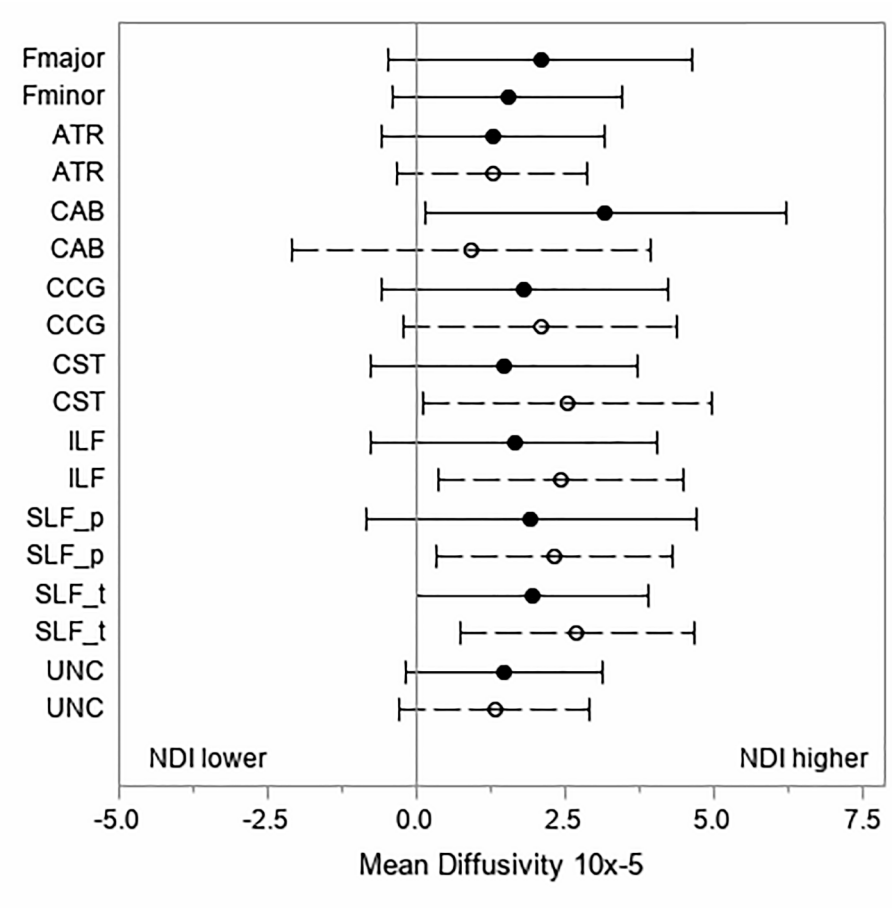

Fig. 2. Mean difference in mean diffusivity (MD) between children with neurodevelopmental impairment (NDI) compared to children without neurodevelopmental impairment. Solid lines/solid circles = left hemisphere; broken lines/open circles = right hemisphere; * = significant following false discovery rate correction. Fmajor = forceps major; fminor = forceps minor; ATR = anterior thalamic radiation; CAB = cingulum angular bundle; CCG = cingulum cingulate gyrus; ILF = inferior longitudinal fasciculus; SLF_p = superior longitudinal fasciculus parietal bundle; SLF_t = superior longitudinal fasciculus temporal bundle; UNC = uncinate fasciculus.

analysis. Children with NDI (n = 38) had a lower birth weight, higher CRIB-II scores and were more likely to live in more deprived areas at the time of assessment (Table 1). The 100 children included in the analysis did not differ in baseline characteristics from the 29 children not included.

3.1. MRI measures and neurodevelopmental impairment

Children with NDI had smaller total brain volumes than those without impairment (Table 2). They also had smaller absolute cortical grey matter and cerebral white matter volumes but not when adjusted for total brain volume. Associations seen between NDI and subcortical grey matter and estimated total intracranial volume were not statistically significant after FDR correction for multiple comparisons.

Children with NDI also had widespread differences in white matter microstructure (Table 3), including lower FA in the corticospinal tract of the right hemisphere, and the uncinate, parietal and temporal regions of the superior longitudinal fasciculi in both hemispheres (Fig. 1). They had higher RD in the same regions and also in the inferior longitudinal fasciculus of the right hemisphere (Fig. 3), and higher MD in the temporal region of the superior longitudinal fasciculus of the right hemisphere (Fig. 2). There were no differences between groups in AD (Fig. 4). The results were similar when children with PVL or IVH grade III/IV were excluded (Supplementary Tables 1 and 2).

3.2. MRI measures and specific functions

MABC-2 scores were positively associated with FA in the uncinate of the left hemisphere and the temporal region of the superior longitudinal fasciculus of the right hemisphere, and negatively associated with RD in the uncinate of the left hemisphere, the temporal and parietal regions of the superior longitudinal fasciculus and the corticospinal tract of the right hemisphere (Table 5). Additionally, MABC-2 scores were positively associated with cortical grey matter volume, but this was not statistically significant after correction for multiple comparison (Table 4).

There was no association between WISC scores and DTI measures following correction for multiple comparisons (Table 5). WISC scores were negatively associated with ventricle volume and positively associated with subcortical grey matter volume, but findings were no longer statistically significant after multiple comparison correction (Table 4). Additionally, there was no association between WISC scores and volume measures when children with PVL or IVH grade III/IV were excluded. All other results for both continuous measures remained the same in the sensitivity analyses (Supplementary Tables 3 and 4).

3.3. Exploratory analyses

When a binary measure of neonatal hyperglycaemia was included in the model as an interaction term, there was no significant interaction between neonatal hyperglycaemia and the relationship between MRI measures and NDI.

4. Discussion

Approximately 30 percent of individuals born very preterm will experience physical or cognitive impairment (Blencowe et al., 2013) and preterm birth is associated with altered brain development. (de Kieviet et al., 2012; Li et al., 2015) We investigated the MRI correlates of NDI in 7-year-old children who were born before 30 weeks' gestation or had very low birthweight (<1500 g). Altered white matter microstructure was observed in several major white matter tracts in children with NDI, including the corticospinal tract, the uncinate and the superior

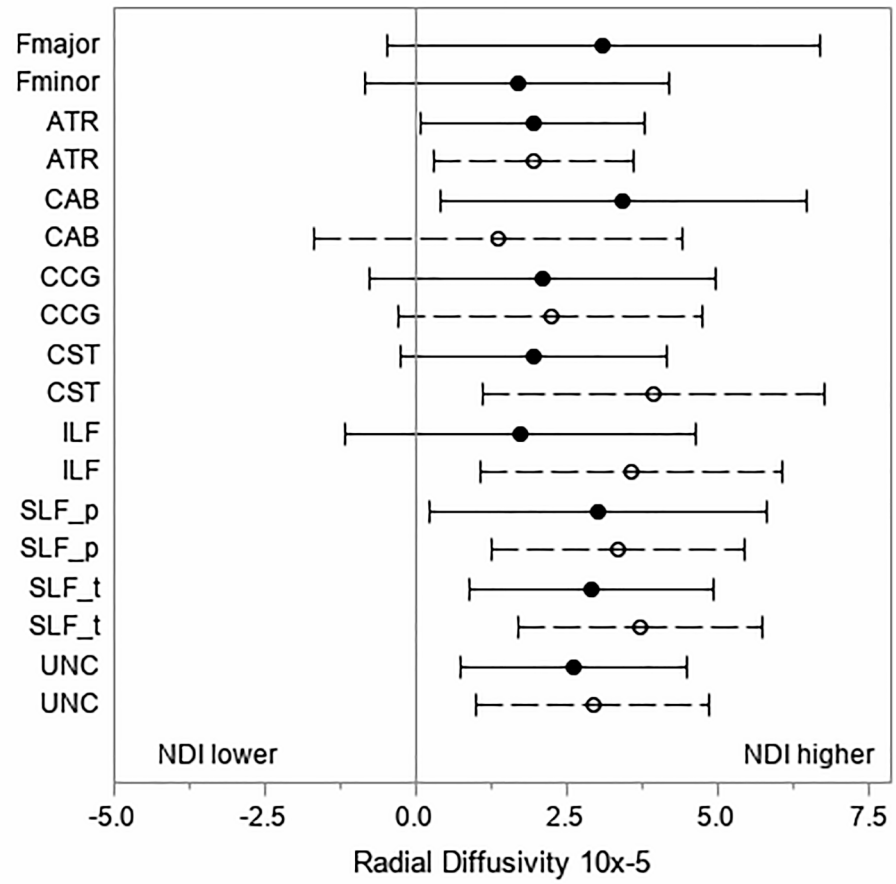

Fig. 3. Mean difference in radial diffusivity (RD) between with neurodevelopmental impairment (NDI) compared to children without neurodevelopmental impairment. Solid lines/solid circles = left hemisphere; broken lines/open circles = right hemisphere; * = significant following false discovery rate correction. Fmajor = forceps major; fminor = forceps minor; ATR = anterior thalamic radiation; CAB = cingulum angular bundle; CCG = cingulum cingulate gyrus; ILF = inferior longitudinal fasciculus; SLF_p = superior longitudinal fasciculus parietal bundle; SLF_t = superior longitudinal fasciculus temporal bundle; UNC = uncinate fasciculus.

longitudinal fasciculus. Additionally, children with NDI had smaller total brain volumes and correspondingly smaller volumes of cerebral white matter and cortical grey matter. These relationships were not altered by neonatal hyperglycaemia and not explained by perinatal brain injury.

We found that in children with NDI, lower FA was coupled with higher RD, but no difference in AD. Age-related increasing FA or decreasing MD is often accompanied by decreasing RD, whereas the findings for changes in AD have been less consistent. (Lebel et al., 2019) Multiple maturation processes in white matter such as increasing membrane density and decreasing brain water content, extracellular distance and membrane permeability result in higher FA and lower diffusivity measures as the brain develops. (Dubois et al., 2014) This makes it difficult to reliably interpret the biological processes underlying the DTI differences seen here. For example, RD has been linked with myelin loss, (Song et al., 2005, 2002) extracellular volume and axon spacing, (Schwartz et al., 2005) while AD has been linked with axonal content (Song et al., 2005, 2002) and axon diameter, (Schwartz et al., 2005) although both measures are related to axon count and myelin volume fraction. (Schwartz et al., 2005) Previously it has been suggested that individuals born VPT have delayed myelination relative to full-term individuals based on higher RD coupled with a higher orientation dispersion index. (Young et al., 2019). Recent research using two MRI techniques with high myelin specificity, magnetisation transfer ratio and T1-weighted/T2-weighted (T1-w/T2-w) ratio, found widespread differences throughout the brain in four-year-old children born < 32 weeks compared to children born full term suggesting delayed myelination (Vandewouw et al., 2019). Furthermore, T1-w/T2-w ratio in eleven major white matter tracts was positively associated with IQ, language and visual-motor integration, indicating that more mature myelination was linked with better performance on these measures (Vandewouw et al., 2019). While it is possible that neurodevelopmental impairment may be related to differences in myelination or axonal packing in our population, DTI parameters lack the specificity to separate these processes. Furthermore, MRI at multiple timepoints is necessary to determine whether brain maturation processes in children with NDI are "delayed", implying a subsequent catch up, or if there are differences in the neural architecture that remain stable over time.

Our findings suggest that NDI are related to DTI differences observed in the corticospinal tract, the uncinate fasciculus and the superior longitudinal fasciculus; regions where lower FA was previously reported in VPT children compared to full-term children (Vollmer et al., 2017; Duerden et al., 2013). In our cohort, the relationships with DTI measures were stronger for motor function than for IQ in these three white matter tracts. This is similar to another report that poorer motor scores were related to increased diffusivity in regional parcellations that included corticospinal and superior longitudinal fibres in 7 year old children born VPT (Thompson et al., 2014). The corticospinal tract extends from the motor cortex through the midbrain and brain stem and is known to be key for motor function. Four components have been proposed to make up the superior longitudinal fasciculus, two of which were delineated in this study: a parietal and a temporal bundle (Yendiki et al., 2011). The parietal bundle corresponds to the superior longitudinal fasciculus III which extends to the premotor regions; it is important for executive functions and is thought to provide somatosensory input to the premotor regions (Makris et al., 20052005). The temporal bundle closely relates to the arcuate fasciculus. In a study of language ability in children born < 32 weeks, earlier gestation at birth and lower linguistic and cognitive performance at age 2 years was linked with lower FA in the arcuate fasciculus at term equivalent age, while cognitive performance at 2 years was also positively associated with FA in the rest of the superior longitudinal fasciculi (Salvan et al., 2017). The uncinate fasciculus has also

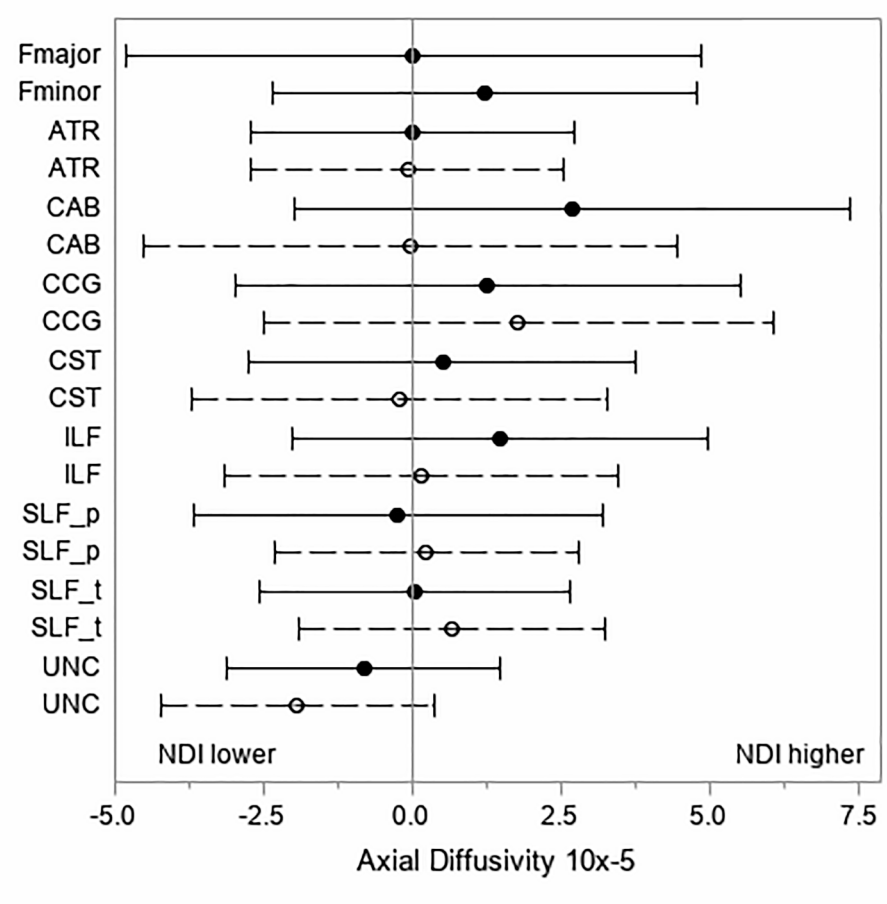

Fig. 4. Mean difference in axial diffusivity (AD) between children with neurodevelopmental impairment (NDI) compared to children without neurodevelopmental impairment. Solid lines/solid circles = left hemisphere; broken lines/open circles = right hemisphere. Fmajor = forceps major; fminor = forceps minor; ATR = anterior thalamic radiation; CAB = cingulum angular bundle; CCG = cingulum cingulate gyrus; ILF = inferior longitudinal fasciculus; SLF_p = superior longitudinal fasciculus parietal bundle; SLF_t = superior longitudinal fasciculus temporal bundle; UNC = uncinate fasciculus.

Table 4
Association between brain volumes and continuous measures of motor function and IQ.

	M−ABC (n = 96)		Adjusted for TBV		WISC (n = 100)		Adjusted for TBV	
	mm^3 (95% CI)	*p*		*p*	mm^3 (95% CI)	*p*	mm^3 (95% CI)	*p*
eTIV	1,501 (−464 to 3,466)	0.133	–	–	1,710 (−413 to 3,833)	0.113	–	–
TBV	1,452 (−137 to 3,041)	0.073	–	–	1,188 (−513 to 2,890)	0.169	–	–
Ventricles	−13 (−201 to 175)	0.889	−40 (−230 to 150)	0.678	−448 (−781 to −115)	0.009	−468 (−805 to −131)	0.007
Cortical GM	966 (49 to 1883)	0.039	181 (−147 to 509)	0.277	825 (−172 to 1822)	0.104	177 (−194 to 549)	0.346
Subcortical GM	23 (−37 to 82)	0.454	−17 (−59 to 24)	0.412	68 (4 to 133)	0.039	36 (−10 to 82)	0.123
Cerebral WM	180 (−427 to 787)	0.556	−318 (−591 to −46)	0.023	473 (−181 to 1127)	0.154	73 (−247 to 392)	0.652
Corpus callosum	−0.5 (−8 to 7)	0.884	−4 (−10 to 3)	0.295	−2 (−11 to 6)	0.582	−5 (−13 to 3)	0.246

Data are change in volume associated with increase in neurodevelopmental score Analyses have been adjusted for sex, gestational age at birth, birthweight z-score, age at assessment, multiplicity, New Zealand deprivation index. WISC = Wechsler Intelligence Scale for Children 4th edition; M−ABC = Movement Assessment Battery for Children 2nd edition; eTIV = estimated Total intracranial volume; TBV = total brain volume excluding ventricles; GM = grey matter; WM = white matter

been implicated in language as well as memory and emotion processing as it connects frontal and ipsilateral anterior temporal lobes (Hasan et al., 2009). Major white matter tracts reach peak FA and minimum MD in the third decade of life; however, fronto-temporal connections have the slowest maturation, closely followed by the corticospinal tract (Lebel and Beaulieu, 2011; Lebel et al., 2008, 2012). It is possible that altered maturation seen in these late maturing regions have the most impact on functional outcomes.

Children with NDI had smaller total brain volume, cerebral white matter, and cortical grey matter volumes, although the regional volume differences did not remain significant when adjusted for total brain volume. We expected children with NDI would have smaller subcortical grey matter volume as smaller volumes and abnormalities in this region have been previously cited as critical to neurodevelopmental outcomes at age 7 years following VPT birth (Loh et al., 2017; Omizzolo et al., 2014). However, the difference in subcortical grey matter between the two groups was not robust enough to survive corrections for multiple comparisons, nor did it remain following adjustment for total brain volume. It is possible that we observed fewer volumetric differences between those with and without NDI among children who were all born < 30 weeks gestation than may have been detected had we included a full-term control group, as throughout childhood and adolescence those born preterm consistently have smaller brain volumes than those born at term (de Kieviet et al., 2012; El Marroun et al., 2020). Nonetheless, brain tissue volumes have been positively associated with IQ and motor function in VPT children in other cohorts (Monson et al., 2016; Loh et al., 2017), although these associations were not robust to multiple comparison correction in the current investigation. Furthermore, perinatal brain injury may partly explain these finding in our cohort, as larger ventricle volume and smaller subcortical volume were no longer

Table 5
Association between DTI measures and continuous measure of motor function and IQ.

	M–ABC (n = 72)							
	FA (95% CI) × 10^{-4}	*p*	MD (95% CI) × 10^{-7}	*p*	AD (95% CI) × 10^{-7}	*p*	RD (95% CI) × 10^{-7}	*p*
F major	12.45 (2.43 to 22.47)	0.016	−7.54 (−15.25 to 0.18)	0.055	5.53 (−8.93 to 19.98)	0.447	−14.07 (−24.6 to −3.54)	0.055
F minor	−0.41 (−7.72 to 6.91)	0.912	−5.15 (−10.88 to 0.58)	0.077	−9.09 (−19.38 to 1.2)	0.082	−3.17 (−10.7 to 4.35)	0.077
L ATR	2.42 (−2.09 to 6.94)	0.288	−6.14 (−11.79 to −0.49)	0.034	−6.31 (−14.61 to 1.98)	0.133	−6.06 (−11.79 to −0.32)	0.034
R ATR	2.02 (−2.91 to 6.96)	0.416	−5.45 (−10.29 to −0.61)	0.028	−6.09 (−14.1 to 1.91)	0.133	−5.12 (−10.35 to 0.11)	0.028
L CAB	0.45 (−6.90 to 7.79)	0.904	−7.53 (−17.02 to 1.96)	0.118	−9.86 (−24.24 to 4.52)	0.176	−6.36 (−15.92 to 3.19)	0.118
R CAB	0.17 (−7.02 to 7.37)	0.962	−0.06 (−9.36 to 9.23)	0.989	−0.49 (−14.34 to 13.35)	0.944	0.15 (−9.28 to 9.58)	0.989
L CCG	6.37 (−2.05 to 14.78)	0.135	−8.44 (−15.75 to −1.14)	0.024	−5.27 (−18.24 to 7.71)	0.421	−10.03 (−18.68 to −1.39)	0.024
R CCG	4.03 (−3.44 to 11.51)	0.285	−9.34 (−16.17 to −2.51)	0.008	−9.86 (–22.72 to 2.99)	0.130	−9.07 (−16.26 to −1.89)	0.008
L CST	5.34 (0.68 to 10.00)	0.025	−8.18 (−14.89 to −1.47)	0.018	−6.75 (−16.66 to 3.17)	0.179	−8.9 (−15.5 to −2.29)	0.018
R CST	8.24 (1.58 to 14.90)	0.016	−9.35 (−16.10 to −2.59)	0.007	−4.51 (−15.22 to 6.19)	0.403	**−11.77 (−19.44 to −4.09)**	**0.007***
L ILF	4.08 (−3.21 to 11.37)	0.268	−6.82 (−14.30 to 0.66)	0.073	−5.69 (−16.51 to 5.12)	0.297	−7.38 (−16.38 to 1.62)	0.073
R ILF	8.71 (1.87 to 15.54)	0.013	−6.74 (−13.21 to −0.28)	0.041	−0.30 (−10.56 to 9.96)	0.954	−9.96 (−17.85 to −2.08)	0.041
L SLF – p	4.07 (−1.43 to 9.56)	0.144	−10.37 (−18.60 to −2.13)	0.015	−11.33 (−21.52 to −1.14)	0.030	−9.88 (−18.24 to −1.52)	0.015
R SLF – p	6.14 (1.46 to 10.83)	0.011	−8.57 (−14.66 to −2.48)	0.007	−5.17 (−13.07 to 2.74)	0.196	**−10.27 (−16.68 to −3.86)**	**0.007***
L SLF – t	5.09 (0.20 to 9.97)	0.042	−7.45 (−13.27 to −1.63)	0.013	−5.67 (−13.58 to 2.25)	0.157	−8.33 (−14.57 to −2.1)	0.013
R SLF – t	**6.99 (2.64 to 11.34)**	**0.002***	−8.45 (−14.50 to −2.40)	0.007	−4.30 (−12.2 to 3.60)	0.281	**−10.52 (−16.77 to −4.28)**	**0.007***
L Uncinate	**7.77 (3.01 to 12.54)**	**0.002***	−5.65 (−10.70 to −0.60)	0.029	1.04 (−6.12 to 8.20)	0.772	**−8.99 (−14.72 to −3.26)**	**0.029***
R Uncinate	4.01 (−1.77 to 9.80)	0.171	−2.28 (−7.25 to 2.70)	0.365	1.46 (−5.68 to 8.61)	0.684	−4.14 (−10.42 to 2.13)	0.365
	WISC (n = 73)							
	FA (95% CI) × 10^{-4}	*p*	MD (95% CI) × 10^{-7}	*p*	AD (95% CI) × 10^{-7}	*p*	RD (95% CI) × 10^{-7}	*p*
F major	8.70 (−3.66 to 21.07)	0.164	−6.08 (−15.28 to 3.13)	0.191	0.83 (−16.52 to 18.18)	0.924	−9.53 (–22.47 to 3.41)	0.146
F minor	4.91 (−3.26 to 13.08)	0.234	−3.61 (−10.22 to 2.99)	0.278	0.08 (−11.92 to 12.08)	0.989	−5.46–13.89 to 2.96)	0.200
L ATR	6.67 (1.79 to 11.54)	0.008	−5.66 (−12.08 to 0.77)	0.084	−0.84 (−10.33 to 8.65)	0.860	−8.06 (−14.43 to −1.69)	0.014
R ATR	5.98 (0.60 to 11.36)	0.030	−5.36 (−10.86 to 0.13)	0.056	−1.54 (−10.71 to 7.63)	0.738	−7.28 (−13.06 to −1.50)	0.014
L CAB	7.20 (−1.01 to 15.40)	0.084	−8.71 (−19.38 to 1.96)	0.108	−3.66 (−20.05 to 12.74)	0.658	−11.24 (−21.86 to −0.62)	0.038
R CAB	9.99 (2.26 to 17.71)	0.012	−4.17 (−14.65 to 6.31)	0.430	6.06 (−9.47 to 21.58)	0.439	−9.28 (−19.73 to 1.16)	0.081
L CCG	4.47 (−5.24 to 14.17)	0.362	−6.84 (−15.22 to 1.55)	0.108	−6.15 (−20.90 to 8.59)	0.408	−7.18 (−17.21 to 2.85)	0.158
R CCG	5.62 (−3.43 to 14.66)	0.219	−9.00 (−16.91 to −1.10)	0.026	−8.68 (–23.46 to 6.10)	0.245	−9.16 (−17.86 to −0.47)	0.039
L CST	5.83 (0.57 to 11.10)	0.030	−6.19 (−13.97 to 1.60)	0.117	−3.02 (−14.35 to 8.31)	0.596	−7.77 (−15.41 to −0.14)	0.046
R CST	13.79 (5.86 to 21.72)	0.001	−10.23 (−18.55 to −1.91)	0.017	1.71 (−10.41 to 13.83)	0.779	−16.20 (−25.87 to −6.53)	0.001
L ILF	4.90 (−3.22 to 13.02)	0.232	−6.32 (−14.74 to 2.11)	0.139	−3.57 (−15.81 to 8.66)	0.562	−7.69 (−17.75 to 2.37)	0.132
R ILF	7.38 (−0.48 to 15.24)	0.065	−6.74 (−14.00 to 0.52)	0.068	−1.73 (−13.26 to 9.80)	0.765	−9.25 (−18.22 to −0.28)	0.043
L SLF – p	6.81 (0.21 to 13.40)	0.043	−7.62 (−17.19 to 1.96)	0.117	−3.96 (−15.88 to 7.95)	0.509	−9.44 (−19.20 to 0.32)	0.058
R SLF – p	6.64 (1.04 to 12.24)	0.021	−7.20 (−14.22 to −0.18)	0.045	−2.50 (−11.45 to 6.45)	0.579	−9.55 (−17.08 to −2.02)	0.014
L SLF – t	6.35 (0.85 to 11.85)	0.024	−5.44 (−12.28 to 1.39)	0.117	−1.34 (−10.44 to 7.77)	0.771	−7.50 (−14.76 to −0.24)	0.043
R SLF – t	7.34 (2.25 to 12.44)	0.005	−6.88 (−13.95 to 0.19)	0.056	−1.85 (−10.82 to 7.12)	0.682	−9.40 (−16.79 to −2.01)	0.014
L Uncinate	7.51 (1.94 to 13.08)	0.009	−4.51 (−10.32 to 1.29)	0.125	2.25 (−5.82 to 10.32)	0.579	−7.90 (−14.59 to −1.20)	0.022
R Uncinate	9.18 (2.94 to 15.42)	0.005	−3.58 (−9.19 to 2.03)	0.207	5.92 (−2.14 to 13.97)	0.147	−8.33 (−15.20 to −1.46)	0.018

Data are change in diffusion measures associated with increase in neurodevelopmental score. Analyses have been adjusted for sex, gestational age at birth, birthweight z-score, age at assessment, multiplicity, New Zealand deprivation index. WISC = Wechsler Intelligence Scale for Children 4th edition; FA = fractional anisotropy; MD = mean diffusivity; AD = axial diffusivity; RD = radial diffusivity; ATR = anterior thalamic radiation; CAB = cingulate – angular bundle; CCG = cingulum – cingulate gyrus; CST = corticospinal tract; ILF = inferior longitudinal fasciculus; SLF – p = superior longitudinal fasciculus – parietal; SLF – t = superior longitudinal fasciculus – temporal; Uncinate = uncinate fasciculus; * still statistically supported following FDR correction including all outcomes from Table 4 and Table 5.

related to IQ when children with PVL or IVH grade III or IV were excluded.

One key aim of the PIANO study was to determine the long-term implications of neonatal hyperglycaemia. (Alsweiler et al., 2012). Therefore, we explored the interaction between neonatal hyperglycaemia and the relationship between NDI and brain structure and found that the interaction did not significantly affect the main findings. The rates of children who experienced neonatal hyperglycaemia did not differ between the two NDI groups. Furthermore, the main analyses were extensively adjusted for perinatal factors, suggesting that the observed differences between children with and without NDI are not due to neonatal morbidities.

The cross-sectional design of our study is a limitation. The MRI scans and neurodevelopmental outcomes were collected at a single timepoint, there is some evidence that imaging at term-equivalent age may be more predictive of later outcomes than imaging in mid-childhood (Monson et al., 2016). Multiple timepoints for MRI would be helpful in determining whether brain growth is slower in children with NDI, as has been found in VPT children compared with full term children (Thompson et al., 2020). Furthermore, it is not clear to what extent VPT children without NDI in our cohort are similar to children born at term as there are no normative values for brain maturation and we did not have a control group. Likewise, direct comparison of absolute diffusion values between studies or datasets is not advised as the acquisition parameters directly influence their calculation. (Lebel et al., 2019) Previous studies of white matter alterations in VPT individuals have more commonly used tract-based spatial statistics (TBSS); a voxel-based approach that provides information on the whole-brain white matter. However, TBSS is limited by alignment issues that can lead to anatomical inaccuracies (Bach et al., 2014) and only offers information on a string of voxels within a tract based on the highest FA value. We used a global probabilistic tractography approach to derive diffusion measures of known white matter pathways that overcomes these issues by working in the space of individual participant's neuroanatomy and providing average diffusion values over the entire pathway (Yendiki et al., 2011), although this limited our investigation to ten major white matter tracts.

Overall, this study indicates that in a cohort of 7 year old children born VPT, those with NDI have altered brain structure compared to those without NDI. Children with NDI had smaller total brain volumes and differences in microstructure in three major white matter tracts. Two of these regions, the uncinate and superior longitudinal fasciculi, are the later developing fibres of the brain and one, the corticospinal tract, is fundamental for motor function. Future research employing multiple MRI modalities to interrogate white matter microstructure at multiple timepoints would shed more light on the cellular processes underlying NDI.

Declaration of Competing Interest

The authors declare that they have no known competing financial interests or personal relationships that could have appeared to influence the work reported in this paper.

Acknowledgements

We are extremely grateful to all the families who took part in the PIANO Study. We would also like to thank the PIANO Steering Group for their feedback in all stages of manuscript preparation.

Funding

This study was funded in part by grants from the Gravida: National Centre for Growth and Development (Grant no. 12-MP03), Health Research Council of New Zealand and the A + Trust.

Appendix A. Supplementary data

Supplementary data to this article can be found online at https://doi.org/10.1016/j.nicl.2021.102730.

References

Alsweiler, J.M., Harding, J.E., Bloomfield, F.H., 2012. Tight glycemic control with insulin in hyperglycemic preterm babies: A randomized controlled trial. Pediatrics 129 (4), 639–647. https://doi.org/10.1542/peds.2011-2470.

Bach, M., Laun, F.B., Leemans, A., Tax, C.M.W., Biessels, G.J., Stieltjes, B., Maier-Hein, K. H., 2014. Methodological considerations on tract-based spatial statistics (TBSS). Neuroimage. 100, 358–369. https://doi.org/10.1016/j.neuroimage.2014.06.021.

Benjamini, Y., Hochberg, Y., 1995. Controlling the False Discovery Rate: A Practical and Powerful Approach to Multiple Testing. Source J R Stat Soc Ser B. 57 (1), 289–300. https://doi.org/10.2307/2346101.

Blencowe, H., Cousens, S., Chou, D., Oestergaard, M., Say, L., Moller, A.-B., Kinney, M., Lawn, J., 2013. Born Too Soon: The global epidemiology of 15 million preterm births. Reprod Health. 10 (Suppl 1), S2. https://doi.org/10.1186/1742-4755-10-S1-S2.

Blencowe, H., Lee, A.CC., Cousens, S., Bahalim, A., Narwal, R., Zhong, N., Chou, D., Say, L., Modi, N., Katz, J., Vos, T., Marlow, N., Lawn, J.E., 2013. Preterm birth-associated neurodevelopmental impairment estimates at regional and global levels for 2010. Pediatr. Res. 74 (S1), 17–34. https://doi.org/10.1038/pr.2013.204.

Boardman, J.P., Craven, C., Valappil, S., Counsell, S.J., Dyet, L.E., Rueckert, D., Aljabar, P., Rutherford, M.A., Chew, A.T.M., Allsop, J.M., 2010. A common neonatal image phenotype predicts adverse neurodevelopmental outcome in children born preterm. Neuroimage. 52 (2), 409–414. https://doi.org/10.1016/j.neuroimage.2010.04.261.

Botellero, V.L., Skranes, J., Bjuland, K.J., Håberg, A.K., Lydersen, S., Brubakk, A.-M., Indredavik, M.S., Martinussen, M., 2017. A longitudinal study of associations between psychiatric symptoms and disorders and cerebral gray matter volumes in adolescents born very preterm. BMC Pediatr. 17 (1) https://doi.org/10.1186/s12887-017-0793-0.

Dai, D.W.T., Wouldes, T.A., Brown, G.T.L., Tottman, A.C., Alsweiler, J.M., Gamble, G.D., Harding, J.E., 2020. Relationships between intelligence, executive function and academic achievement in children born very preterm. Early Hum Dev. 148, 105122. https://doi.org/10.1016/j.earlhumdev.2020.105122.

Dale, A.M., Fischl, B., Sereno, M.I., 1999. Cortical surface-based analysis: I. Segmentation and surface reconstruction. *Neuroimage*. 9 (2), 179–194. https://doi.org/10.1006/nimg.1998.0395.

Dale, A.M., Sereno, M.I., 1993. Improved localization of cortical activity by combining EEG and MEG with MRI cortical surface reconstruction: A linear approach. J. Cogn. Neurosci. 5 (2), 162–176. https://doi.org/10.1162/jocn.1993.5.2.162.

de Kieviet JF, Zoetebier L, van ELBURG RM, Vermeulen RJ, Oosterlaan J. Brain development of very preterm and very low-birthweight children in childhood and adolescence: a meta-analysis. Dev. Med. Child. Neurol. 2012;54(4):313-323. doi: 10.1111/j.1469-8749.2011.04216.x.

Dubois, J., Dehaene-Lambertz, G., Kulikova, S., Poupon, C., Hüppi, P.S., Hertz-Pannier, L., 2014. The early development of brain white matter: A review of imaging studies in fetuses, newborns and infants. Neuroscience 276, 48–71. https://doi.org/10.1016/j.neuroscience.2013.12.044.

Duerden, E.G., Card, D., Lax, I.D., Donner, E.J., Taylor, M.J., 2013. Alterations in frontostriatal pathways in children born very preterm. Dev. Med. Child Neurol. 55 (10), 952–958. https://doi.org/10.1111/dmcn.12198.

Duerden, E.G., Foong, J., Chau, V., Branson, H., Poskitt, K.J., Grunau, R.E., Synnes, A., Zwicker, J.G., Miller, S.P., 2015. Tract-based spatial statistics in preterm-born neonates predicts cognitive and motor outcomes at 18 months. Am. J. Neuroradiol. 36 (8), 1565–1571. https://doi.org/10.3174/ajnr.A4312.

El Marroun, H., Zou, R., Leeuwenburg, M.F., Steegers, E.A.P., Reiss, I.K.M., Muetzel, R.L., Kushner, S.A., Tiemeier, H., 2020. Association of Gestational Age at Birth with Brain Morphometry. JAMA Pediatr. 174 (12), 1149. https://doi.org/10.1001/jamapediatrics.2020.2991.

Estep, M.E., Smyser, C.D., Anderson, P.J., Ortinau, C.M., Wallendorf, M., Katzman, C.S., Doyle, L.W., Thompson, D.K., Neil, J.J., Inder, T.E., Shimony, J.S., 2014. Diffusion tractography and neuromotor outcome in very preterm children with white matter abnormalities. Pediatr. Res. 76 (1), 86–92. https://doi.org/10.1038/pr.2014.45.

Fischl, B., Dale, A.M., 2000. Measuring the thickness of the human cerebral cortex from magnetic resonance images. Proc Natl Acad Sci U S A. 97 (20), 11050–11055. https://doi.org/10.1073/pnas.200033797.

Fischl B, Salat DH, Van Der Kouwe AJW, et al. Sequence-independent segmentation of magnetic resonance images. NeuroImage. Vol 23. ; 2004:69-84. doi:10.1016/j.neuroimage.2004.07.016.

Fischl, B., Liu, A., Dale, A.M., 2001. Automated manifold surgery: Constructing geometrically accurate and topologically correct models of the human cerebral cortex. IEEE Trans. Med. Imaging. 20 (1), 70–80. https://doi.org/10.1109/42.906426.

Fischl, B., Salat, D.H., Busa, E., Albert, M., Dieterich, M., Haselgrove, C., van der Kouwe, A., Killiany, R., Kennedy, D., Klaveness, S., Montillo, A., Makris, N., Rosen, B., Dale, A.M., 2002. Whole brain segmentation: Automated labeling of neuroanatomical structures in the human brain. Neuron 33 (3), 341–355. https://doi.org/10.1016/S0896-6273(02)00569-X.

Hasan, K.M., Iftikhar, A., Kamali, A., Kramer, L.A., Ashtari, M., Cirino, P.T., Papanicolaou, A.C., Fletcher, J.M., Ewing-Cobbs, L., 2009. Development and aging of the healthy human brain uncinate fasciculus across the lifespan using diffusion tensor tractography. Brain Res. 1276, 67–76. https://doi.org/10.1016/j.brainres.2009.04.025.

Jones, D.K., Knösche, T.R., Turner, R., 2013. White matter integrity, fiber count, and other fallacies: The do's and don'ts of diffusion MRI. Neuroimage. 73, 239–254. https://doi.org/10.1016/j.neuroimage.2012.06.081.

Kuperberg, G.R., Broome, M.R., McGuire, P.K., David, A.S., Eddy, M., Ozawa, F., Goff, D., West, W.C., Williams, S.C.R., van der Kouwe, A.J.W., Salat, D.H., Dale, A.M., Fischl, B., 2003. Regionally localized thinning of the cerebral cortex in schizophrenia. Arch. Gen. Psychiatry 60 (9), 878. https://doi.org/10.1001/archpsyc.60.9.878.

Lax, I.D., Duerden, E.G., Lin, S.Y., Mallar Chakravarty, M., Donner, E.J., Lerch, J.P., Taylor, M.J., 2013. Neuroanatomical consequences of very preterm birth in middle childhood. Brain Struct. Funct. 218 (2), 575–585. https://doi.org/10.1007/s00429-012-0417-2.

Lebel, C., Beaulieu, C., 2011. Longitudinal development of human brain wiring continues from childhood into adulthood. J. Neurosci. 31 (30), 10937–10947. https://doi.org/10.1523/JNEUROSCI.5302-10.2011.

Lebel, C., Walker, L., Leemans, A., Phillips, L., Beaulieu, C., 2008. Microstructural maturation of the human brain from childhood to adulthood. Neuroimage. 40 (3), 1044–1055. https://doi.org/10.1016/j.neuroimage.2007.12.053.

Lebel, C., Gee, M., Camicioli, R., Wieler, M., Martin, W., Beaulieu, C., 2012. Diffusion tensor imaging of white matter tract evolution over the lifespan. Neuroimage. 60 (1), 340–352. https://doi.org/10.1016/j.neuroimage.2011.11.094.

Lebel, C., Treit, S., Beaulieu, C., 2019. A review of diffusion MRI of typical white matter development from early childhood to young adulthood. NMR Biomed. 32 (4), e3778. https://doi.org/10.1002/nbm.v32.410.1002/nbm.3778.

Li, K.e., Sun, Z., Han, Y., Gao, L., Yuan, L.i., Zeng, D., 2015. Fractional anisotropy alterations in individuals born preterm: A diffusion tensor imaging meta-analysis. Dev. Med. Child Neurol. 57 (4), 328–338. https://doi.org/10.1111/dmcn.2015.57.issue-410.1111/dmcn.12618.

Loh, W.Y., Anderson, P.J., Cheong, J.L.Y., Spittle, A.J., Chen, J., Lee, K.J., Molesworth, C., Inder, T.E., Connelly, A., Doyle, L.W., Thompson, D.K., 2017. Neonatal basal ganglia and thalamic volumes: Very preterm birth and 7-year neurodevelopmental outcomes. Pediatr. Res. 82 (6), 970–978. https://doi.org/10.1038/pr.2017.161.

Lund, L.K., Vik, T., Lydersen, S., Løhaugen, G.CC., Skranes, J., Brubakk, A.-M., Indredavik, M.S., 2012. Mental health, quality of life and social relations in young adults born with low birth weight. Health Qual Life Outcomes. 10 (1), 146. https://doi.org/10.1186/1477-7525-10-146.

Makris N, Kennedy DN, McInerney S, et al. Segmentation of subcomponents within the superior longitudinal fascicle in humans: A quantitative, in vivo, DT-MRI study. Cereb Cortex. 2005;15(6):854-869. doi:10.1093/cercor/bhh186.

Monson, B.B., Anderson, P.J., Matthews, L.G., Neil, J.J., Kapur, K., Cheong, J.L.Y., Doyle, L.W., Thompson, D.K., Inder, T.E., 2016. Examination of the pattern of growth of cerebral tissue volumes from hospital discharge to early childhood in very preterm infants. JAMA Pediatr. 170 (8), 772. https://doi.org/10.1001/jamapediatrics.2016.0781.

Murray, A.L., Thompson, D.K., Pascoe, L., Leemans, A., Inder, T.E., Doyle, L.W., Anderson, J.F.I., Anderson, P.J., 2016. White matter abnormalities and impaired attention abilities in children born very preterm. Neuroimage. 124, 75–84. https://doi.org/10.1016/j.neuroimage.2015.08.044.

O'Donnell, L.J., Westin, C.F., 2011. An introduction to diffusion tensor image analysis. Neurosurg. Clin. N. Am. 22 (2), 185–196. https://doi.org/10.1016/j.nec.2010.12.004.

Omizzolo, C., Scratch, S.E., Stargatt, R., Kidokoro, H., Thompson, D.K., Lee, K.J., Cheong, J., Neil, J., Inder, T.E., Doyle, L.W., Anderson, P.J., 2014. Neonatal brain abnormalities and memory and learning outcomes at 7 years in children born very preterm. Memory. 22 (6), 605–615. https://doi.org/10.1080/09658211.2013.809765.

Pascal, A., Govaert, P., Oostra, A., Naulaers, G., Ortibus, E., Van den Broeck, C., 2018. Neurodevelopmental outcome in very preterm and very-low-birthweight infants born over the past decade: a meta-analytic review. Dev. Med. Child. Neurol. 60 (4), 342–355. https://doi.org/10.1111/dmcn.2018.60.issue-410.1111/dmcn.13675.

Petrou, S., Khan, K., 2012. Economic costs associated with moderate and late preterm birth: Primary and secondary evidence. Semin Fetal Neonatal Med. 17 (3), 170–178. https://doi.org/10.1016/j.siny.2012.02.001.

Reuter, M., Rosas, H.D., Fischl, B., 2010. Highly accurate inverse consistent registration: A robust approach. Neuroimage. 53 (4), 1181–1196. https://doi.org/10.1016/j.neuroimage.2010.07.020.

Rosas, H.D., Liu, A.K., Hersch, S., Glessner, M., Ferrante, R.J., Salat, D.H., van der Kouwe, A., Jenkins, B.G., Dale, A.M., Fischl, B., 2002. Regional and progressive thinning of the cortical ribbon in Huntington's disease. Neurology. 58 (5), 695–701. https://doi.org/10.1212/WNL.58.5.695.

Salvan, P., Tournier, J.D., Batalle, D., Falconer, S., Chew, A., Kennea, N., Aljabar, P., Dehaene-Lambertz, G., Arichi, T., Edwards, A.D., Counsell, S.J., 2017. Language ability in preterm children is associated with arcuate fasciculi microstructure at term. Hum. Brain Mapp. 38 (8), 3836–3847. https://doi.org/10.1002/hbm.23632.

Schwartz, E.D., Cooper, E.T., Fan, Y., Jawad, A.F., Chin, C.-L., Nissanov, J., Hackney, D. B., 2005. MRI diffusion coefficients in spinal cord correlate with axon morphometry. NeuroReport 16 (1), 73–76. https://doi.org/10.1097/00001756-200501190-00017.

Ségonne, F., Dale, A.M., Busa, E., Glessner, M., Salat, D., Hahn, H.K., Fischl, B., 2004. A hybrid approach to the skull stripping problem in MRI. Neuroimage. 22 (3), 1060–1075. https://doi.org/10.1016/j.neuroimage.2004.03.032.

Ségonne, F., Pacheco, J., Fischl, B., 2007. Geometrically accurate topology-correction of cortical surfaces using nonseparating loops. IEEE Trans. Med. Imaging 26 (4), 518–529. https://doi.org/10.1109/TMI.2006.887364.

Sled, J.G., Zijdenbos, A.P., Evans, A.C., Sied, J.G., Zijdenbos, A.P., Evans, A.C., 1998. A nonparametric method for automatic correction of intensity nonuniformity in mri data. IEEE Trans. Med. Imaging 17 (1), 87–97. https://doi.org/10.1109/42.668698.

Smith, S.M., 2002. Fast robust automated brain extraction. Hum. Brain Mapp. 17 (3), 143–155. https://doi.org/10.1002/(ISSN)1097-019310.1002/hbm.v17:310.1002/hbm.10062.

Song, S.K., Sun, S.W., Ramsbottom, M.J., Chang, C., Russell, J., Cross, A.H., 2002. Dysmyelination revealed through MRI as increased radial (but unchanged axial) diffusion of water. Neuroimage. 17 (3), 1429–1436. https://doi.org/10.1006/nimg.2002.1267.

Song, S.-K., Yoshino, J., Le, T.Q., Lin, S.-J., Sun, S.-W., Cross, A.H., Armstrong, R.C., 2005. Demyelination increases radial diffusivity in corpus callosum of mouse brain. Neuroimage. 26 (1), 132–140. https://doi.org/10.1016/j.neuroimage.2005.01.028.

Thompson, D.K., Lee, K.J., Egan, G.F., Warfield, S.K., Doyle, L.W., Anderson, P.J., Inder, T.E., 2014. Regional white matter microstructure in very preterm infants: Predictors and 7 year outcomes. Cortex. 52, 60–74. https://doi.org/10.1016/j.cortex.2013.11.010.

Thompson, D.K., Matthews, L.G., Alexander, B., Lee, K.J., Kelly, C.E., Adamson, C.L., Hunt, R.W., Cheong, J.L.Y., Spencer-Smith, M., Neil, J.J., Seal, M.L., Inder, T.E., Doyle, L.W., Anderson, P.J., 2020. Tracking regional brain growth up to age 13 in children born term and very preterm. Nat. Commun. 11 (1) https://doi.org/10.1038/s41467-020-14334-9.

Tottman AC, Bloomfield FH, Cormack BE, et al. Relationships Between Early Nutrition and Blood Glucose Concentrations in Very Preterm Infants. J. Pediatr. Gastroenterol. Nutr. 2018;66(6):960-966. doi:10.1097/MPG.0000000000001929.

Travis, K.E., Adams, J.N., Ben-Shachar, M., Feldman, H.M., Gong, G., 2015. Decreased and increased anisotropy along major cerebral white matter tracts in preterm children and adolescents. PLoS ONE 10 (11), e0142860. https://doi.org/10.1371/journal.pone.0142860.

Vandewouw, M.M., Young, J.M., Shroff, M.M., Taylor, M.J., Sled, J.G., 2019. Altered myelin maturation in four year old children born very preterm. NeuroImage Clin. 21, 101635. https://doi.org/10.1016/j.nicl.2018.101635.

Vollmer, B., Lundequist, A., Mårtensson, G., Nagy, Z., Lagercrantz, H., Smedler, A.-C., Forssberg, H., Baud, O., 2017. Correlation between white matter microstructure and executive functions suggests early developmental influence on long fibre tracts in preterm born adolescents. PLoS ONE 12 (6), e0178893. https://doi.org/10.1371/journal.pone.0178893.

Yendiki, A., Panneck, P., Srinivasan, P., et al., 2011. Automated probabilistic reconstruction of white-matter pathways in health and disease using an atlas of the underlying anatomy. Front Neuroinform. 5, 23. https://doi.org/10.3389/fninf.2011.00023.

Young, J.M., Vandewouw, M.M., Morgan, B.R., Lou, S.M., Sled, J.G., Taylor, M.J., 2018. Altered white matter development in children born very preterm. Brain Struct. Funct. 223 (5), 2129–2141. https://doi.org/10.1007/s00429-018-1614-4.

Young, J.M., Vandewouw, M.M., Mossad, S.I., Morgan, B.R., Lee, W., Smith, M.L., Sled, J. G., Taylor, M.J., 2019. White matter microstructural differences identified using multi-shell diffusion imaging in six-year-old children born very preterm. NeuroImage Clin. 23, 101855. https://doi.org/10.1016/j.nicl.2019.101855.